EVALUATION OF THEORETICAL MODELS FOR PREDICTING THERMAL CONDUCTIVITY OF BO CHINH GINSENG ROOT BASED ON EXPERIMENTAL DATA

Nguyen Hay[1], Nguyen The Bao[2,3], Ngo Thi Minh Hieu[4,5,*], Le Quang Huy[5]

DOI: https://doi.org/10.57001/huih5804.2026.135

ABSTRACT

Thermal conductivity is an important thermophysical property in the simulation of freezing and freeze-drying processes of biological materials. This study evaluates the predictive performance of thermal conductivity models for Bo Chinh ginseng root (*Abelmoschus sagittifolius*) over the temperature range from -30 to 30°C by comparing several commonly used theoretical models with previously published experimental data. The models examined include the parallel and series bounds, Maxwell-Eucken, effective medium theory (EMT), Levy (1981), and the co-continuous model proposed by Wang (2008). Statistical analysis indicates that the Wang model provides the best agreement with experimental measurements, yielding MAE and RMSE values of 0.028 and 0.031W/m·K, respectively, whereas models based on single continuous-phase assumptions or idealized geometric configurations exhibit larger deviations, particularly in the frozen region. The results suggest that model accuracy is strongly influenced by the underlying structural assumptions, with the co-continuous approach offering improved representation of heat transfer behavior in heterogeneous materials. The findings provide a basis for selecting appropriate models in thermal calculations and process simulations involving Bo Chinh ginseng root.

Keywords: *Bo Chinh ginseng root; Thermal conductivity; Theoretical models; Freezing; Heterogeneous biological materials*

[1]Faculty of Vehicle and Energy Engineering, Ho Chi Minh City University of Technology and Engineering, Vietnam
[2]Faculty of Mechanical Engineering, Ho Chi Minh City University of Technology (HCMUT), Vietnam
[3]Faculty of Mechanical Engineering, University of Technology - Vietnam National University Ho Chi Minh City (VNU-HCM), Vietnam
[4]Faculty of Engineering and Technology, Nong Lam University, Vietnam
[5]Faculty of Heat and Refrigeration Technology, Cao Thang Technical College, Vietnam
[*]Email: ngothiminhhieu@caothang.edu.vn
Received: 20/3/2026
Revised: 10/5/2026
Accepted: 25/5/2026

1. INTRODUCTION

Thermal conductivity is a key thermophysical property governing heat transfer mechanisms during food preservation and processing, particularly in freezing and freeze-drying operations. For high-value medicinal materials such as Bo Chinh ginseng (*Abelmoschus sagittifolius*), accurate determination of thermophysical properties is essential not only for optimizing process efficiency but also for preserving valuable bioactive compounds, including saponins. According to Nguyen *et al.* [1], Bo Chinh ginseng cultivated in Vietnam exhibits a complex biological structure composed of multiple constituents such as water, proteins, lipids, carbohydrates, and ash.

During freezing, thermal conductivity directly controls the rate of heat transfer, thereby influencing freezing time and temperature distribution within the material. In the phase transition region, the transformation of water from liquid to solid causes significant changes in thermal conductivity, since the thermal conductivity of ice is

substantially higher than that of liquid water [2-5]. In heat transfer simulations of freezing processes, thermal conductivity serves as a critical input parameter, and the accuracy of numerical predictions depends strongly on the reliability of this property, particularly for heterogeneous biological materials [6, 7].

Although thermal conductivity can be determined experimentally, such measurements require specialized equipment and involve considerable technical challenges, especially under subzero temperature conditions. Consequently, theoretical models have been widely employed to estimate thermal conductivity based on material composition.

Currently, numerous theoretical approaches have been proposed to predict the effective thermal conductivity of materials with different structural characteristics. For materials with complex microstructures such as biological tissues, frozen foods, and porous media, Wang *et al.* [8] combined several theoretical models, including the parallel, series, Maxwell-Eucken, and Effective Medium Theory (EMT) models, to predict thermal conductivity. Subsequently, Wang *et al.* [9] applied a co-continuous model coupled with EMT to estimate thermal conductivity of ice chips and synthetic snow.

In addition, several studies have evaluated the deviation between model predictions and experimental measurements of thermal conductivity, notably the work reported by Hoang *et al.* [10]. However, these investigations have mainly focused on animal-based materials. Carson *et al.* [11] analyzed theoretical models to identify those providing the highest accuracy for predicting thermal conductivity of isotropic materials based on composition and temperature, but their study was limited to materials such as meat, fish, ice cream, and powders, without considering plant-based materials.

Systematic studies assessing the applicability and limitations of theoretical models for Bo Chinh ginseng over a wide temperature range remain scarce. Therefore, the objective of this study is to quantitatively evaluate the performance of the parallel, series, Maxwell-Eucken 1 and 2, Effective Medium Theory, Levy (1981), and Wang (2008) models in predicting the thermal conductivity of Bo Chinh ginseng root over the temperature range from –30 to 30°C. The novelty of this work lies in the combined comparison of model predictions with experimental data obtained using the transient hot-wire method, together with microstructural analysis based on scanning electron microscopy (SEM), thereby clarifying the relationship between the actual material microstructure and the underlying assumptions of the theoretical models.

2. MATERIALS AND METHODS

2.1. Experimental data source

The experimental data used to validate the theoretical models in this study were obtained from independent measurements conducted by the authors using the transient hot wire method (Figure 1) [12]. Measurements were performed over a wide temperature range from -30 to 30°C, with each temperature condition measured in triplicate, and the results reported as mean values accompanied by standard deviations. Owing to the short heating duration, this method minimizes the influence of material heterogeneity and ensures reliable thermal conductivity measurements for biological samples. In the present study, experimental data were employed as reference values to evaluate the predictive performance and applicability limits of the theoretical models.

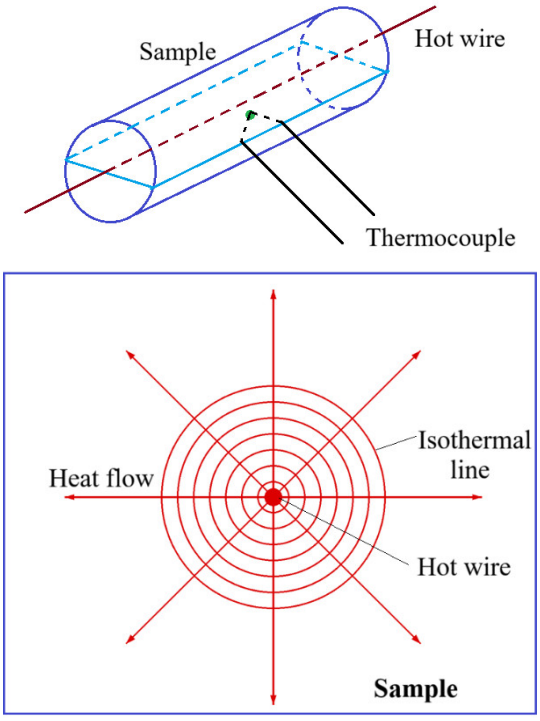

Figure 1. Transient hot wire method [12]

The experimental dataset utilized in this work was previously published by the authors and is adopted here as benchmark data for model validation.

2.2. Material composition

The composition of fresh Bo Chinh ginseng root was analyzed at the Saigon High-Tech Analytical Center (SAIGONSTC). The analytical results, including protein, fat,

carbohydrate, fiber, and ash contents, are presented in Table 1 and were used to estimate the solid phase fraction in the heat transfer models.

Table 1. Component of fresh Ginseng (according to SAIGONSTC)

Component	Protein	Fat	Carbohydrate	Fiber	Ash
Percentage (%)	1.4	0.3	14.7	1.63	1.52

2.3. Ice fraction calculation

The model proposed by Tchigeov was employed to determine the fraction of frozen water as a function of temperature. This model has been reported to be applicable to various biological materials and was shown to provide good accuracy according to the evaluation of Fricke and Becker [3]. The frozen water fraction was calculated using the following expression:

$$x_{ice} = \frac{1.105 x_{w0}}{1 + \frac{0.7138}{\ln(t_f - t + 1)}} \quad (1)$$

Where:

x_{ice}: Mass fraction of ice

x_{wo}: Mass fraction of water in the unfrozen material

t: Temperature (°C)

t_f: Initial freezing temperature of water in the material (°C).

The ice fraction as a function of temperature was calculated and summarized in Table 2.

Table 2. Ice fraction of Bo Chinh ginseng root as a function of temperature

Temperature, °C	-30	-25	-20	-15	-10	-5	-4	-3	-2	0
Ice fraction (%)	73.4	72.7	71.7	70.2	67.6	60.8	57.5	51.7	37.9	0

2.4. Initial freezing temperature and initial moisture content of the material

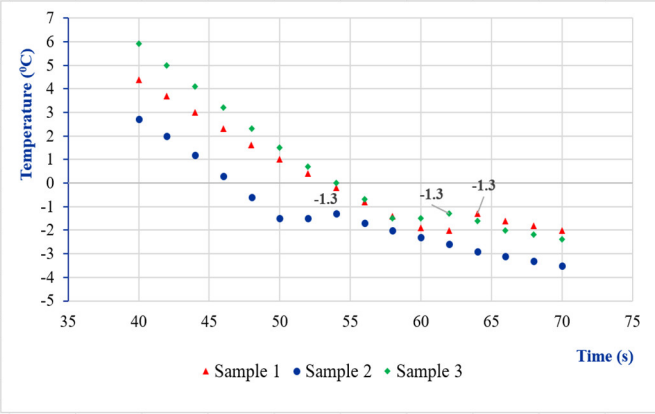

Figure 2. Initial freezing temperature of the material determined experimentally

The initial freezing temperature of moisture in Bo Chinh ginseng root was experimentally determined as t_f = -1.3°C This value was used as the threshold to distinguish between the unfrozen and frozen states of the material.

The initial moisture content of the ginseng root was determined using an infrared moisture analyzer (Kett FD-720, Japan), yielding an average value of 79% on a wet basis. This value was used to estimate the water content and solid phase fraction of the material as a function of temperature.

2.5. Theoretical models

In this work, theoretical models for predicting effective thermal conductivity were selected to represent the ginseng root as a multiphase system. The parallel and series models, following the approach of Murakami and Okos, were employed to define the physical limits of thermal conductivity. In addition, semi-theoretical models, including the Maxwell–Eucken models (ME1 and ME2), effective medium theory (EMT), the Levy (1981) model [13], and the co-continuous structural model proposed by Wang *et al.* [7], were applied to account for the influence of phase distribution and the water-ice phase transition on thermal conductivity. The Choi and Okos model was used to determine the temperature-dependent thermal conductivity of individual components, which were subsequently used as input parameters in the above models [14]. Comparison between model predictions and experimental data enabled assessment of the applicability and limitations of each model under different temperature conditions. To support model application, the phase composition of the material was first defined as described below.

The phases present in the material were determined based on its composition as well as their temperature-dependent phase behavior. The solid phase was taken to include protein, fat, carbohydrates, fiber, and ash, according to the compositional analysis results shown in Table 1. The water content was obtained from the measured moisture content. When the temperature drops below 0°C, the total water was further separated into ice and unfrozen water fractions. This separation was estimated using the model proposed by Tchigeov, with the corresponding values summarized in Table 2. With this treatment, the material can be described as a three-

phase system - ice, unfrozen water, and solid matter - before any further simplification or phase reduction is applied.

In the frozen region (t < 0°C), the material exists as a multiphase system consisting of ice, unfrozen water, and solid matter. However, several theoretical models employed in this study, including the Maxwell-Eucken, effective medium theory (EMT), and Levy (1981) models, are inherently formulated for two-phase systems. Therefore, prior to their application, the three-phase structure was simplified into an equivalent two-phase representation. In contrast, the parallel and series models, as well as the co-continuous model proposed by Wang *et al.* [7], can be directly applied to multiphase systems without requiring phase reduction.

The phase reduction from a three-phase to a two-phase system was performed by grouping components with similar thermal roles into an effective phase. In the present study, unfrozen water and solid matter were combined into a single equivalent dispersed phase, while ice was treated as the second phase. The effective thermal conductivity of the combined phase was determined based on the volume fractions of its constituents. This approach preserves the dominant contrast in thermal conductivity between ice and the remaining components, which is a key factor governing heat transfer in frozen materials.

The Choi and Okos model [14] was used to determine the thermal conductivity of individual components as a function of temperature, as presented in the following Table 3.

2.5.1. Murakami and Okos model

Murakami and Okos proposed simple structural models to estimate the effective thermal conductivity of foods and heterogeneous biological materials. In the present study, two basic configurations, namely the parallel and series models, were employed to represent the extreme physical bounds of thermal conductivity for multiphase materials.

In the parallel model, the phases are assumed to be arranged parallel to the direction of heat transfer. The effective thermal conductivity is determined as follows:

$$k_{par} = \sum x_i^v k_i \quad (2)$$

The volume fraction of component i was determined from its mass fraction and density, and x_i^v was calculated as follows:

$$x_i^v = \frac{\frac{x_i}{\rho_i}}{\sum \frac{x_i}{\rho_i}} \quad (3)$$

Where:

k: Thermal conductivity of the material (W/m.K)

k_i: Thermal conductivity of the ith component (W/m.K)

x_i: Mass fraction of the ith component

ρ_i: Density of the ith component (kg/m^3)

x_i^v: Volume fraction of the ith component

This model generally yields the maximum value of effective thermal conductivity and represents the upper bound. In contrast, the series model assumes that the phases are arranged perpendicular to the direction of heat transfer. The effective thermal conductivity is determined as follows:

$$k_{per} = \frac{1}{\sum \frac{x_i^v}{k_i}} \quad (4)$$

This model yields the minimum value of thermal conductivity and is considered the lower bound. The two

Table 3. Thermophysical properties of food components ($-40^0C \le t \le 150^0C$), according to Choi and Okos [14]

Components	Thermal conductivity, k W/(m.K)	Density, ρ (kg/m^3)
Protein	$1.7881\ 10^{-1} + 1.1958 \times 10^{-3}t - 2.7178 \times 10^{-6}t^2$	$1.3299 \times 10^3 - 5.1840 \times 10^{-1}t$
Fat	$1.8071 \times 10^{-1} - 2.7604 \times 10^{-3}t - 1.7749 \times 10^{-7}t^2$	$9.2559 \times 10^2 - 4.1757 \times 10^{-1}t$
Carbohydrate	$2.0141 \times 10^{-1} + 1.3874 \times 10^{-3}t - 4.3312 \times 10^{-6}t^2$	$1.5991 \times 10^3 - 3.1046 \times 10^{-1}t$
Fiber	$1.8331 \times 10^{-1} + 1.2497 \times 10^{-3}t - 3.1683 \times 10^{-6}t^2$	$1.3115 \times 10^3 - 3.6589 \times 10^{-1}t$
Ash	$3.2962 \times 10^{-1} + 1.4011 \times 10^{-3}t - 2.9069 \times 10^{-6}t^2$	$2.4238 \times 10^3 - 3.1046 \times 10^{-1}t$
Water	$5.7109 \times 10^{-1} + 1.7625 \times 10^{-3}t - 6.7036 \times 10^{-6}t^2$	$9.9718 \times 10^2 + 3.1439 \times 10^{-3}t - 3.7574 \times 10^{-3}t^2$
Ice	$2.2196 - 6.2489 \times 10^{-3}t + 1.0154 \times 10^{-4}t^2$	$9.1689 \times 10^2 - 1.3071 \times 10^{-1}t$

Murakami and Okos models were employed as bounding models to define the range of effective thermal conductivity. For biological materials such as ginseng root, particularly under freezing conditions where solid, liquid water, and ice phases coexist, these models serve as reference limits for comparison with more advanced theoretical approaches.

2.5.2. Maxwell-Eucken models (ME1 and ME2)

The Maxwell-Eucken model assumes that one phase forms a continuous matrix while the other phase exists as discrete dispersed inclusions [15]. Depending on which phase is considered continuous, two configurations of the Maxwell-Eucken model are defined. Maxwell-Eucken 1 (ME1) is applied when phase 1 is treated as the continuous matrix and phase 2 as the dispersed phase, whereas Maxwell-Eucken 2 (ME2) represents the opposite configuration.

The effective thermal conductivity is determined by using the following expressions, respectively:

$$k_{ME1} = k_1 \frac{k_2 + 2k_1 + 2v_2(k_2 - k_1)}{k_2 + 2k_1 - v_2(k_2 - k_1)} \quad (5)$$

$$k_{ME2} = k_2 \frac{k_1 + 2k_2 + 2v_1(k_1 - k_2)}{k_1 + 2k_2 - v_1(k_1 - k_2)} \quad (6)$$

Where k_1 and k_2 are the thermal conductivities of the two phases, and v_1 and v_2 are the corresponding volume fractions.

For material temperatures above 0°C, the ME1 configuration was applied to determine thermal conductivity, with liquid water treated as the continuous phase and solids as the dispersed phase. Conversely, in the subzero temperature region (t < 0°C), the ME2 configuration was adopted, in which ice was assumed to be the continuous phase, while the dispersed phase consisted of a mixture of dry matter and unfrozen water.

Since ME1 and ME2 were employed over different temperature ranges, the thermal conductivity predicted by the Maxwell-Eucken model is denoted collectively as k_{ME}, where k_{ME} is calculated using ME1 for t > 0°C and ME2 for t < 0°C.

2.5.3. Effective Medium Theory (EMT)

The Effective Medium Theory (EMT), also referred to as the Bruggeman model, assumes that the phases within the material are randomly distributed and that each phase is embedded in a homogeneous effective medium whose thermal conductivity is equal to the effective thermal conductivity of the entire material [15]. The effective thermal conductivity of the material according to the EMT model is determined from the following equation:

$$v_1 \frac{k_1 - k_{EMT}}{k_1 + 2k_{EMT}} + v_2 \frac{k_2 - k_{EMT}}{k_2 + 2k_{EMT}} = 0 \quad (7)$$

Where k_1 and k_2 are the thermal conductivities of the two phases, and v_1 and v_2 are the corresponding volume fractions.

In the unfrozen temperature region, phase 1 corresponds to liquid water and phase 2 represents solid matter. In the frozen temperature region, phase 1 is ice, while phase 2 consists of unfrozen water and solid matter.

2.5.4. Levy (1981) model

Levy [10] proposed a theoretical model to estimate the effective thermal conductivity of heterogeneous materials, in which the material is treated as a uniform, isotropic two-phase system with heat transfer dominated by conduction. The thermal conductivity of the material according to the Levy model is determined using the following expression:

$$k_{Levy} = \frac{k_2\left[\left(2 + \frac{k_1}{k_2}\right) + 2\left(\frac{k_1}{k_2} - 1\right)F\right]}{\left(2 + \frac{k_1}{k_2}\right) - \left(\frac{k_1}{k_2} - 1\right)F} \quad (8)$$

Where k_1 and k_2 are the thermal conductivities of components 1 and 2, respectively, and F is a structural parameter that reflects the influence of phase morphology and spatial distribution within the material.

The parameter F_1 was proposed by Levy as follows:

$$F_1 = 0.5\left\{\left(\frac{2}{\sigma} - 1 + 2R_1\right) - \left[\left(\frac{2}{\sigma} - 1 + 2R_1\right)^2 - \frac{8R_1}{\sigma}\right]^{0.5}\right\} \quad (9)$$

Where:

$$\sigma = \frac{\left(\frac{k_1}{k_2} - 1\right)^2}{\left(\frac{k_1}{k_2} + 1\right)^2 + \frac{1}{2}\frac{k_1}{k_2}} \quad (10)$$

Where R_1 is the volume fraction of component 1.

$$R_1 = \left[1 + \left(\frac{1}{x_1} - 1\right)\left(\frac{\rho_1}{\rho_2}\right)\right]^{-1} \quad (11)$$

where x_1 is the mass fraction of component 1, ρ_1 is the density of component 1, and ρ_2 is the density of component 2.

Compared with bounding models such as the parallel and series configurations, the Levy model accounts for the influence of microstructural characteristics on heat transfer, particularly under conditions of large contrasts in thermal conductivity between phases

2.5.5. Co-continuous model of Wang et al. (2008)

Wang *et al.* [7] proposed a co-continuous model to estimate the effective thermal conductivity of heterogeneous materials, based on a combination of the two limiting heat transfer mechanisms represented by the parallel and series configurations. The effective thermal conductivity of the material is determined using the following expression:

$$k_{Wang} = \frac{1}{2}\sum_i \frac{x_i^v}{k_i}\left(\sqrt{1+\frac{8\sum_i k_i x_i^v}{\sum_i \frac{x_i^v}{k_i}}}-1\right) \quad (12)$$

In the above expression, the summation term $\sum k_i x_i^v$ represents the parallel heat transfer mechanism, whereas the product term $\sum \frac{x_i^v}{k_i}$ reflects the perpendicular heat transfer mechanism.

This model allows a continuous transition between the two extreme heat transfer limits without requiring prior assumptions about a specific microstructural arrangement and is therefore particularly suitable for heterogeneous biological materials exhibiting large contrasts in thermal conductivity between phases.

2.6. Computational workflow

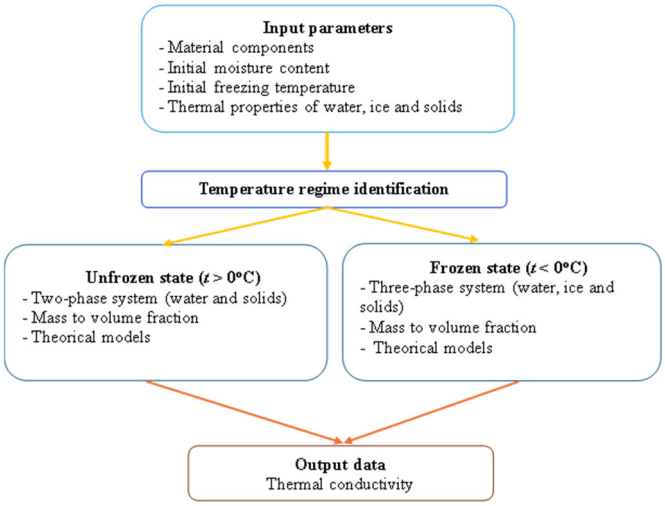

Figure 3. Flowchart illustrates the computational procedure for determining the effective thermal conductivity of ginseng root under unfrozen and frozen conditions

Figure 3 presents the computational workflow for predicting thermal conductivity as a function of temperature. Material composition and temperature were first used to determine phase mass and volume fractions. The material was treated as a two-phase system for $t > 0$°C and as a three-phase system for $t < 0$°C. For models formulated for two-phase systems, including the Maxwell-Eucken, EMT, and Levy models, the three-phase structure in the frozen region was simplified into an equivalent two-phase representation. In contrast, the parallel and series models, as well as the Wang (2008) model, were applied directly without requiring phase reduction. The models were then used to estimate $k(T)$, and the calculated results were compared with experimental data to evaluate the accuracy of each model.

2.7. Statistical error analysis

To evaluate the agreement between predicted values and experimental data over the entire temperature range from -30 to 30°C, the relative error (ER), root mean square error (RMSE) and mean absolute error (MAE) were employed. These error metrics were calculated using the following expressions [16]:

$$ER_i = \frac{k_{model,i} - k_{exp,i}}{k_{exp,i}} \times 100\% \quad (13)$$

$$MAE = \frac{1}{n}\sum_{i=1}^{n}\left|k_{model,i} - k_{exp,i}\right| \quad (14)$$

$$RMSE = \sqrt{\frac{1}{n}\sum_{i=1}^{n}\left(k_{model,i} - k_{exp,i}\right)^2} \quad (15)$$

Where:

$k_{model,i}$: the thermal conductivity predicted by the model at the i-th data point,

$k_{exp,i}$: the experimentally determined thermal conductivity at the i-th data point

n: the total number of data points.

3. RESULTS AND DISCUSSION

The variation in thermal conductivity with temperature is primarily governed by the phase transition of water and the associated change in ice fraction. As the temperature decreases below the initial freezing point, the progressive formation of ice leads to a marked increase in thermal conductivity, owing to the significantly higher thermal conductivity of ice compared to liquid water. This behavior indicates that ice fraction plays an important role in controlling heat transfer in the

Table 4. Thermal conductivity of Bo Chinh ginseng root predicted by different models

Temperature *t* (°C)	Parallel model	Perpendicular model	Maxwell -Eucken model	EMT model	Wang (2008) model	Levy (1981) model
	k_par (W/m.K)	*k_per* (W/m.K)	*k_ME* (W/m.K)	*k_EMT* (W/m.K)	*k_Wang* (W/m.K)	*k_Levy* (W/m.K)
-30	2.066	0.788	1.621	1.519	1.741	1.668
-25	2.007	0.805	1.565	1.482	1.697	1.601
-20	1.949	0.817	1.503	1.443	1.656	1.530
-15	1.886	0.822	1.432	1.399	1.619	1.443
-10	1.812	0.816	1.339	1.34	1.582	1.325
-5	1.688	0.780	1.185	1.219	1.536	1.091
0	0.522	0.458	0.478	0.51	0.771	0.635
5	0.531	0.468	0.486	0.518	0.778	0.645
10	0.538	0.477	0.493	0.526	0.784	0.654
15	0.546	0.485	0.501	0.534	0.790	0.664
20	0.554	0.494	0.508	0.541	0.795	0.673
25	0.561	0.502	0.515	0.548	0.800	0.681
30	0.568	0.510	0.522	0.555	0.805	0.689

frozen region. In addition, the strong contrast in thermal conductivity between ice and the remaining components introduces pronounced heterogeneity in the material, which must be properly accounted for in the predictive models.

The thermal conductivity of the material predicted by the theoretical models is presented in the following Table 4.

In the subzero temperature region, thermal conductivity decreases gradually as temperature approaches the initial freezing point, followed by a sharp drop in the phase transition region and a slight increase in the positive temperature range. All theoretical models capture this overall trend; however, their agreement with experimental data differs markedly. The parallel and series models provide the upper and lower bounds, respectively, while semi-empirical models such as Maxwell-Eucken, Wang, Levy, and Effective Medium Theory (EMT) yield predictions lying between these limits. Among them, the Wang and Levy models exhibit better agreement with experimental measurements, particularly in the temperature range below 0°C, where moisture in the material has transitioned to the ice phase. The EMT model tends to underestimate thermal conductivity but still reproduces the thermal transition associated with the liquid-solid phase change of moisture. These results indicate that consideration of microstructural characteristics and phase distribution plays a critical role in predicting heat transfer properties of biological materials during freezing.

The theoretical models selected in this study were applied to predict the effective thermal conductivity of ginseng root under both unfrozen and frozen conditions. Comparison between predicted values and experimental data enables assessment of each model's capability to describe temperature-dependent thermal conductivity and clarifies the differences between bounding models and advanced structural models.

Table 5 compares the deviations between theoretical model predictions and experimental data. The parallel and series models act as bounding models, with average errors of 23.3% and 42.5%, respectively, indicating that these two models mainly provide upper and lower reference limits for thermal conductivity due to their idealized structural assumptions. The Maxwell–Eucken and EMT models yield average errors of 23% and 22.1%, respectively, reflecting the limitations of these approaches arising from their assumptions of ideal phase distributions. In contrast, the Wang model exhibits the highest accuracy over the investigated temperature range, with an average error of only 2.9%, followed by the Levy model with an error of 11.8%. In the temperature region below 0°C, where moisture in the material transitions to the solid phase, the Wang model shows the

Table 5. Comparison between experimentally measured thermal conductivity of Bo Chinh ginseng root and values predicted by theoretical models

t (°C)	k_exp	k_par	ER (%)	k_per	ER (%)	*k_ME*	ER (%)	*k_EMT*	ER (%)	k_Wang	ER (%)	k_Levy	ER (%)
-30	1.716	2.066	20.4	0.788	54.1	1.621	5.5	1.519	11.5	1.741	1.5	1.668	2.8
-25	1.684	2.007	19.2	0.805	52.2	1.565	7.1	1.482	12.0	1.697	0.8	1.601	4.9
-20	1.624	1.949	20.0	0.817	49.7	1.503	7.5	1.443	11.1	1.656	2.0	1.530	5.8
-15	1.614	1.886	16.8	0.822	49.1	1.432	11.3	1.399	13.3	1.619	0.3	1.443	10.6
-10	1.547	1.812	17.2	0.816	47.3	1.339	13.4	1.34	13.4	1.582	2.3	1.325	14.4
-5	1.495	1.688	12.9	0.780	47.8	1.185	20.7	1.219	18.5	1.536	2.7	1.091	27.0
0	0.718	0.522	27.3	0.458	36.2	0.478	33.4	0.51	29.0	0.771	7.4	0.635	11.6
5	0.733	0.531	27.6	0.468	36.2	0.486	33.7	0.518	29.3	0.778	6.1	0.645	12.0
10	0.758	0.538	29.0	0.477	37.1	0.493	35.0	0.526	30.6	0.784	3.4	0.654	13.7
15	0.76	0.546	28.1	0.485	36.1	0.501	34.1	0.534	29.7	0.790	3.9	0.664	12.7
20	0.768	0.554	27.9	0.494	35.7	0.508	33.9	0.541	29.6	0.795	3.6	0.673	12.4
25	0.777	0.561	27.8	0.502	35.4	0.515	33.7	0.548	29.5	0.800	3.0	0.681	12.4
30	0.796	0.568	28.7	0.510	36.0	0.522	34.4	0.555	30.3	0.805	1.1	0.689	13.4

Note:

k_exp: thermal conductivity determined experimentally

k_par: thermal conductivity predicted by the parallel model

k_per: thermal conductivity predicted by the perpendicular model

k_ME: thermal conductivity predicted by Maxwell – Eucken models

k_EMT: thermal conductivity predicted by the Effective Medium Theory (EMT) model

k_Wang: thermal conductivity predicted by the Wang (2008) model

k_Levy: thermal conductivity predicted by the Levy (1981) model

closest agreement with experimental measurements. These results indicate that accounting for microstructural characteristics and phase interactions plays a decisive role in predicting heat transfer properties of biological materials during freezing.

The comparison trends observed in this study are consistent with the findings reported by Hoang *et al.* [10]. In that work, when evaluating thermal conductivity models for various materials over a wide temperature range, the Wang (2008) model yielded the lowest average error of 8.3%, followed by the Levy (1981) model at 10.4%, the EMT model at 13.6%, the parallel model at 23.6%, while the series model exhibited the largest deviation at 35.1%.

The differences in prediction accuracy among the models can be understood in relation to their underlying structural assumptions. Models such as Maxwell–Eucken and effective medium theory, which are based on a single continuous phase with dispersed inclusions, tend to oversimplify the actual microstructure and therefore exhibit larger deviations, particularly in the frozen region. In contrast, the Wang (2008) model provides better agreement with experimental data, as it allows for co-continuous heat transfer pathways and captures the simultaneous contribution of ice and solid phases. This is consistent with the observed microstructure, where ice formation leads to interconnected conductive networks rather than isolated inclusions. The largest discrepancies between model predictions and experimental data are observed near the initial freezing temperature, where rapid changes in ice fraction result in strongly nonlinear variations in thermal conductivity, posing challenges for simplified theoretical approaches.

Results from Table 6 indicate that the Wang (2008) model provides the highest agreement with experimental data, with MAE and RMSE values of 0.028 and 0.031W/m.K, respectively, outperforming the other models. This improved accuracy can be attributed to the co-continuous structural assumption, which allows heat resistance to be represented through both series and

Table 6. Summary of statistical errors of theoretical models compared with experimental data

Models	Wang (2008) model	Levy (1981) model	Maxwell-Eucken model	EMT model	Parallel model	Perpendicular model
MAE (W/m.K)	0.028	0.130	0.219	0.220	0.247	0.521
RMSE (W/m.K)	0.031	0.158	0.228	0.221	0.253	0.587

parallel mechanisms within the material. In contrast, the parallel and series bounding models only represent upper and lower limits based on idealized geometric configurations, resulting in large deviations with RMSE values of 0.253 and 0.587W/m.K, respectively.

The Maxwell-Eucken and EMT models also exhibit relatively high errors, with RMSE values of approximately 0.221 and 0.228W/m.K, owing to their assumption of a single continuous matrix phase with the remaining phases treated as discrete inclusions. This assumption limits their ability to capture the complex heat conduction pathways formed by the simultaneous connectivity of multiple phases in the material. The Levy (1981) model yields intermediate performance (RMSE = 0.1579W/m·K), indicating an improvement over the bounding models but still failing to fully represent heat transfer mechanisms in the multiphase system. Overall, the combined MAE and RMSE metrics demonstrate that model accuracy is strongly governed by the underlying structural assumptions.

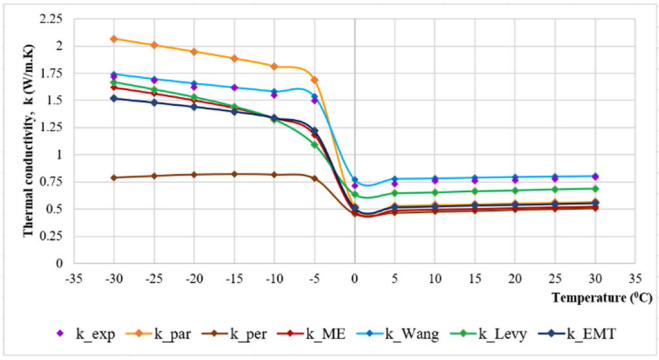

Figure 4. Comparison of temperature-dependent thermal conductivity between theoretical models and experimental data

Figure 4 provides a visual comparison between experimentally measured thermal conductivity and values predicted by theoretical models as a function of temperature. In the subzero temperature region, crystallization of moisture within the material leads to a significant increase in thermal conductivity due to the much higher thermal conductivity of ice compared to liquid water. As temperature decreases, the ice fraction increases, resulting in a continued rise in thermal conductivity. In contrast, in the temperature range above 0°C, water exists entirely in the liquid phase, and variations in thermal conductivity with temperature become negligible due to the relatively small contributions of other material components.

For the bounding models, the parallel model consistently yields the highest values, based on the assumption that constituent phases are arranged parallel to the heat flow direction, leading to minimum thermal resistance. Conversely, the series model produces the lowest values, as it assumes phases are arranged perpendicular to heat flow, resulting in very high thermal resistance. The large deviations of these models from experimental measurements indicate that the microstructure of ginseng root cannot be represented as simple layered arrangements but rather as a complex multiphase system.

The Maxwell-Eucken model provides more accurate predictions than the parallel and series bounds, particularly in the subzero temperature region. However, its accuracy deteriorates significantly at temperatures above 0°C. This behavior is likely due to the assumption of a single continuous phase with the remaining phases treated as dispersed inclusions, which does not fully capture the complex microstructure of biological materials.

The EMT model reproduces the general trend of thermal conductivity variation with temperature; however, substantial discrepancies remain between predicted and experimental values, especially in the positive temperature region where moisture remains in the liquid state. The EMT model exhibits improved performance in the subzero region, where moisture undergoes phase transition to ice.

The Levy (1981) model shows a noticeable improvement in accuracy compared to the bounding models by assuming the material as a homogeneous multiphase system. Nevertheless, it exhibits relatively large errors in the frozen region, with deviations increasing as temperature decreases, reaching approximately 27% at -5°C. This may be attributed to limitations in the model's continuous-phase assumption, which does not adequately represent the formation of

complex ice networks during phase transition in biological materials.

Among all models considered, the Wang (2008) model demonstrates the lowest deviation from experimental data across the investigated temperature range. Its superior performance arises from the ability to combine parallel and series heat transfer mechanisms without imposing a fixed microstructural configuration. The co-continuous framework of the Wang model effectively captures the formation of interconnected ice crystal networks and solid-phase linkages in ginseng root, thereby improving prediction accuracy of thermophysical properties during freezing. To further elucidate the physical mechanisms underlying the differences in model performance, the microstructure of fresh ginseng root was examined using scanning electron microscopy (SEM).

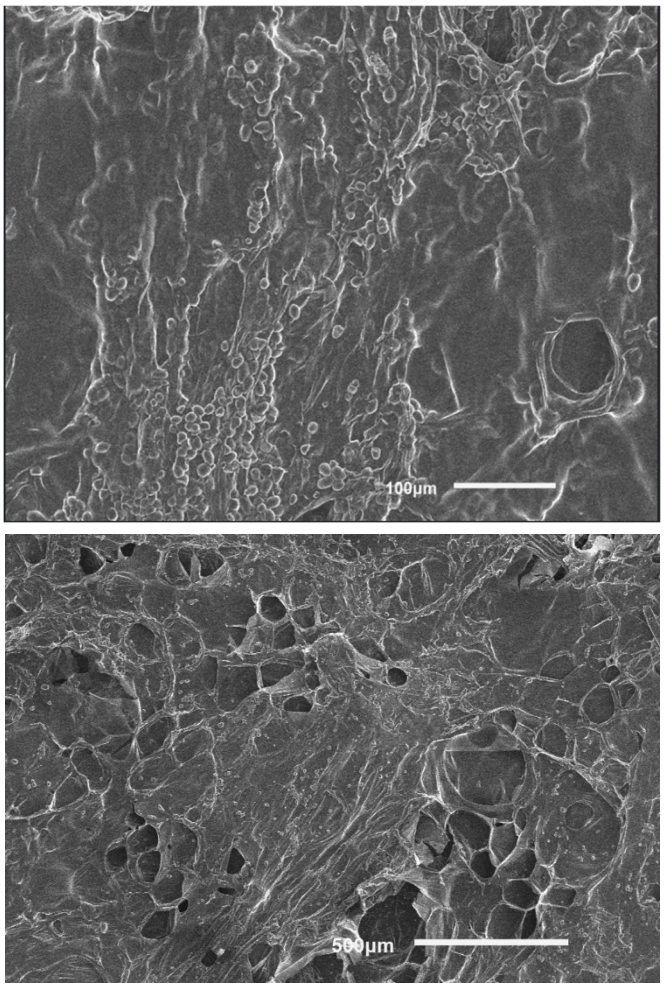

Figure 5. SEM images of the surface microstructure of fresh Bo Chinh ginseng root (magnifications of 100 µm and 500µm)

The SEM images (Figure 5) indicate that the microstructure of Bo Chinh ginseng root consists of a porous cellular network, where the solid cell walls form a continuous framework surrounding interconnected void spaces. These voids, which initially contain liquid water, are likely to be progressively filled with ice during freezing. As this occurs, an additional pathway for heat transfer may develop within the material, meaning that both the solid matrix and the ice phase can participate in heat conduction through connected regions.

Given this structure, heat transfer does not seem to occur through a single dominant phase. Instead, it is more reasonable to consider a combination of parallel and series conduction pathways. This interpretation aligns with the model proposed by Wang *et al.* [7], which allows for co-continuous phases and multiple heat transfer routes. By comparison, models that assume a single continuous phase with dispersed inclusions, or rely on simplified geometric limits, tend to struggle to capture this level of structural complexity, which may explain their larger deviations from experimental observations.

It is also observed that prediction errors tend to increase near the initial freezing point. This can be linked to the rapid change in ice fraction during the phase transition of water, leading to strong nonlinearity of thermal conductivity. In addition, the fibrous and potentially anisotropic nature of the ginseng root may further affect the results, since most theoretical models assume uniform and isotropic phase distributions.

4. CONCLUSION

This study evaluated several theoretical models for predicting the thermal conductivity of Bo Chinh ginseng root over the temperature range from –30 to 30°C using previously published experimental data. Among the models considered, the co-continuous model of Wang (2008) provided the best agreement with measurements, yielding MAE and RMSE values of 0.028W/m.K and 0.031W/m.K, respectively. Models based on single continuous-phase assumptions or idealized geometric limits exhibited larger deviations, particularly in the frozen region. These results indicate that model accuracy is strongly influenced by the underlying structural assumptions rather than the mathematical form of the equations. Overall, the Wang model appears to be the most suitable among those examined for estimating thermal conductivity in heterogeneous biological materials and may serve as a reliable input for simulations of freezing and freeze-drying processes.

REFERENCES

[1]. P. L. Nguyen, Y. L. Ho, V. M. Le, M. Heinrich, Y. S. Chang, "The Vietnamese medicinal and food plant *Abelmoschus sagittifolius* (Kurz.) Merr., an underestimated resource," *Industrial Crops & Products*, 216, Art. no. 118690, 2024.

[2]. ASHRAE, *Refrigeration.* Atlanta, GA, *USA:* American Society of Heating, Refrigerating and Air-Conditioning Engineers, 2022.

[3]. B. A. Fricke, B. R. Becker, "Evaluation of thermophysical property models for foods," *HVAC&R Research*, 7, 4, 311–330, 2001.

[4]. V. R. N. Telis, J. Telis-Romero, P. J. A. Sobral, A. L. Gabas, "Freezing point and thermal conductivity of tropical fruit pulps: Mango and papaya," *International Journal of Food Properties*, 10, 1, 73-84, 2007.

[5]. J. K. Carson, "Review of effective thermal conductivity models for foods," *International Journal of Refrigeration*, 29, 6, 958–967, 2006

[6]. F. P. Incropera, D. P. DeWitt, T. L. Bergman, A. S. Lavine, *Fundamentals of Heat and Mass Transfer,* 6th ed. Hoboken, NJ, USA: John Wiley & Sons, 2007.

[7]. J. F. Wang, J. K. Carson, M. F. North, D. J. Cleland, "A new structural model of effective thermal conductivity for heterogeneous materials with co-continuous phases," *International Journal of Heat and Mass Transfer*, 49, 3075-3083, 2008.

[8]. J. Wang, J. K. Carson, M. F. North, D. J. Cleland, "A new approach to modelling the effective thermal conductivity of heterogeneous materials," *International Journal of Heat and Mass Transfer*, 49, 17-18, 3075-3083, 2006

[9]. J. F. Wang, J. K. Carson, J. Willix, M. F. North, D. J. Cleland, "Application of a co-continuous composite model of effective thermal conductivity to ice-air systems," *International Journal of Refrigeration*, 32, 556-561, 2009

[10]. D. K. Hoang, S. J. Lovatt, J. R. Olatunji, J. K. Carson, "Improved prediction of thermal properties of refrigerated foods," *Journal of Food Engineering*, 297, Art. no. 110485, 2021.

[11]. J. K. Carson, J. Wang, M. F. North, D. J. Cleland, "Effective thermal conductivity prediction of foods using composition and temperature data," *Journal of Food Engineering*, 175, 65-73, 2016.

[12]. M. Mukama, A. Ambaw, U. L. Opara, "Thermophysical properties of fruit-a review with reference to postharvest handling," *J. Food Meas. Charact.*, 14, 6, 2917–2937, 2020.

[13]. F. L. Levy, "A modified Maxwell-Eucken equation for calculating the thermal conductivity of two-component solutions or mixtures," *International Journal of Refrigeration*, 4, 4, 223-225, 1981.

[14]. Y. Choi, M. R. Okos, "Effects of temperature and composition on the thermal properties of foods," *Food Engineering and Process Applications*, 1, 93-101, 1986.

[15]. B. Sundén, J. Yuan, "Evaluation of models of the effective thermal conductivity of porous materials relevant to fuel cell electrodes," *International Journal of Computational Methods and Experimental Measurements*, 1, 4, 440-455, 2013.

[16]. T. O. Hodson, "Root-mean-square error (RMSE) or mean absolute error (MAE): when to use them or not," *Geoscientific Model Development*, 15, 5481-5487, 2022.